LYMPHOID NEOPLASIA

# Sirtuin and pan-class I/II deacetylase (DAC) inhibition is synergistic in preclinical models and clinical studies of lymphoma

Jennifer E. Amengual,[1] Sean Clark-Garvey,[1] Matko Kalac,[1] Luigi Scotto,[1] Enrica Marchi,[2] Ellen Neylon,[1] Paul Johannet,[1] Ying Wei,[3] Jasmine Zain,[1] and Owen A. O'Connor[1]

[1]Center for Lymphoid Malignancies, Columbia University, New York, NY; [2]Department of Medicine, Lincoln Medical Center, New York, NY; and [3]Mailman School of Public Health, Columbia University, New York, NY

## Key Points

- Treatment of DLBCL with the combination of sirtuin and DAC inhibitors leads to synergistic cytotoxicity and acetylation of Bcl6 and p53.
- The overall response rate of relapsed lymphoma patients treated with vorinostat and niacinamide was 24%, and an additional 57% achieved stable disease.

**Understanding the molecular pathogenesis of lymphoma has led to paradigm-changing treatment opportunities. One example involves tailoring specific agents based on the cell of origin in aggressive lymphomas. Germinal center (GC)-derived diffuse large B-cell lymphoma (DLBCL) is known to be driven by an addiction to Bcl6, whereas the activated B-cell (ABC) subtype is driven by nuclear factor κB. In the GC subtype, there is a critical inverse relationship between Bcl6 and p53, the functional status of which is linked to each transcription factor's degree of acetylation. Deacetylation of Bcl6 is required for its transcriptional repressor effects allowing for the oncogene to drive lymphomagenesis. Conversely, acetylation of p53 is activating when class III deacetylases (DACs), or sirtuins, are inhibited by niacinamide. Treatment of DLBCL cell lines with pan-DAC inhibitors in combination with niacinamide produces synergistic cytotoxicity in GC over ABC subtypes. This correlated with acetylation of both Bcl6 and p53. This combination also produced remissions in a spontaneous aggressive B-cell lymphoma mouse model expressing Bcl6. In a phase 1 proof-of-principle clinical trial, 24% of patients with relapsed or refractory lymphoma attained a response to vorinostat and niacinamide, and 57% experienced disease stabilization. We report herein on the preclinical and clinical activity of this targeted strategy in aggressive lymphomas. This trial was registered at www.clinicaltrials.gov as #NCT00691210. (*Blood*. 2013;122(12):2104-2113)**

## Introduction

Understanding the molecular pathogenesis of lymphoma has led to paradigm-changing treatment opportunities. Classification of diffuse large B-cell lymphoma (DLBCL) based on gene expression profiling and cell of origin has created remarkable opportunities to tailor treatment to the molecular phenotype.[1,2] *BCL6* is an oncogene that functions as a transcriptional repressor.[3,4] Dysregulation of *BCL6* in germinal center (GC)–derived DLBCL causes constitutive activation of Bcl6, which downregulates essential tumor suppressors, like p53, and DNA-damage-sensing proteins such as ATR.[5-9] Posttranslational modifications (phosphorylation, acetylation, and ubiquitination) influence the activity of many transcription factors including Bcl6, p53, Hsp90, and nuclear factor κB (NF-κB).[10-14] In the GC, there is a critical inverse relationship between Bcl6 and p53, the functional status of which is linked to each transcription factor's degree of acetylation. Deacetylation of Bcl6 is required for maintaining its effects as a transcriptional repressor; acetylation of Bcl6 disrupts binding of the corepressor MTA3, allowing upregulation of Blimp1 facilitating GC-B-cell differentiation.[15,16] Additionally, Bcl6 directly binds to the promoter region and represses p53 expression in GC B cells.[5]

Class III deacetylases (DAC) inhibitors, known as sirtuin inhibitors, enforce acetylation and activation of p53.[17] Those studied preclinically include niacinamide, sirtinol, cambinol, tenovin-6, APO-866, and EX527. The most robust experience to date exists for niacinamide.[18-20] Sirtuins are highly conserved enzymes involved in cell survival and metabolism.[21-23] Sirtuin inhibition during genotoxic stress leads to hyperacetylation and activation of p53.[17] All sirtuin enzymes have a requirement for nicotinamide adenine dinucleotide (NAD) for catalysis, in contrast to other DACs. Niacinamide, a derivative of vitamin B3 (niacin), is an end product of the sirtuin-NAD reaction that binds to and inhibits the sirtuin catalytic domain and is a precursor of the NAD synthesis pathway. Niacinamide has not been studied systematically in malignancies.

One therapeutic strategy that could favorably shift the relationship between Bcl6 and p53 is to pharmacologically modify their acetylation state through DAC inhibition. DAC inhibitors used in the clinic are pan-class I/II inhibitors (vorinostat, romidepsin, and panobinostat).[24-28] Although vorinostat and romidepsin have been approved by the US Food and Drug Administration for T-cell lymphomas, these drugs are relatively inactive in B-cell lymphomas.[29] Previous studies by Bereshchenko et al have shown that trichostatin A (a pan-DAC inhibitor used exclusively in the laboratory) and niacinamide can modulate Bcl6 in lymphoma cell lines. Herein we establish proof-of-principle data in both preclinical and clinical

Submitted February 25, 2013; accepted July 25, 2013. Prepublished online as *Blood* First Edition paper, August 2, 2013; DOI 10.1182/blood-2013-02-485441.

The online version of this article contains a data supplement.

The publication costs of this article were defrayed in part by page charge payment. Therefore, and solely to indicate this fact, this article is hereby marked "advertisement" in accordance with 18 USC section 1734.

settings that DAC inhibitors, when used in a rational way, can lead to inactivation of the Bcl6 oncogene and activation of the p53 tumor suppressor protein in a favorable therapeutic direction.

## Methods

### Drug and reagents

The following drugs were obtained for laboratory experiments and from the institutional research pharmacy for the clinical trial: panobinostat (Novartis), vorinostat (Merck), belinostat (CuraGen), romidepsin (Glouchester), and niacinamide (Sigma-Aldrich). Western blot and immunoprecipitation reagents were purchased from Bio-Rad and Invitrogen.

### Cell lines

OCI-Ly1, OCI-Ly7, OCI-Ly10, RIVA, and HBL-1 were grown in Iscove modified Dulbecco medium with 10% fetal bovine serum; Su-DHL2, Su-DHL4, and Su-DHL6 were grown in RPMI medium with 10% fetal bovine serum.

### Cytotoxicity assays

Cytotoxicity was evaluated using Cell-titer-Glo (Promega) as reported previously.[30]

### Flow cytometry

Apoptosis was measured using Yo-Pro-1 and propidium iodide (Vybrant apoptosis assay kit 4; Invitrogen) as previously described.[32]

### Western blotting and immunoprecipitation

Western blotting was performed as previously described.[32] Antibodies used include the following: anti–acetyl-p53 (Lys 382) (Santa Cruz Biotechnology), anti–acetyl-p53 (Lys373, Lys382) (Millipore), anti-p53 DO-1 (Abcam), anti-Blimp1(*N*-20) (Santa Cruz Biotechnology), anti-p21 (Cell Signaling Technology), anti–β-actin (Cell Signaling Technology), anti-Bcl6 (D-8) (Santa Cruz Biotechnology), anti–caspase 3 (Cell Signaling Technology), and anti-PARP (46D11) (Cell Signaling Technology).

For detection of acetylated-Bcl6, $4 \times 10^7$ OCI-Ly1, OCI-Ly7 cells were treated with 1 of 4 pan-DAC inhibitors with or without niacinamide for 3 hours. Immunoprecipitation was performed as previously described[12] with Protein G-Agarose Beads (Santa Cruz Biotechnology). Antibodies used include the following: antiacetylated lysine (Cell Signaling Technology), anti-Bcl6 (D-8) (Santa Cruz Biotechnology), and anti-Bcl6 N3 (Santa Cruz Biotechnology).

Densitometry analysis was performed on scanned immunoblot images using the ImageJ software (National Institutes of Health).

### In vivo tumor model

Animals were housed in a barrier, pathogen-free mouse facility, maintained in accordance with the principles of laboratory animal care under an Institutional Animal Care and Use Committee–approved protocol. Generation of double transgenic CD19-CherryLuciferase crossed with λ-MYC C57BL mice were bred as previously described.[33] Mice were screened twice weekly for tumor growth measured by in vivo bioluminescence imaging utilizing D-luciferin (Caliper Life Sciences, Hopkinton, MA), conducted on a cryogentically cooled In Vivo Imaging System (IVIS) system (Xenogen Corp., Alameda, CA). Image acquisition and measurement of bioluminescence was analyzed using Living Image software (Xenogen) as previously described.[33] Mice were eligible for assignment to 1 of 5 cohorts once they achieved a detectable prespecified bioluminescent signal of $20 \times 10^6$ photons per second per $cm^2$ per sr correlating with 100-mg tumor weight. Mice were divided into 5 cohorts of 5 to 6 mice as follows: (1) control, normal saline daily days 1 through 5; (2) niacinamide (N), 60 mg/kg daily days 1 through 5; (3) romidepsin (R), 1.0 mg/kg day 1 and normal saline days 2 through 5; (4) N + R, N days 1 through 5 and R day 1; and (5) N→R, N days 1 through 5 and R day 3. All drugs were diluted in normal saline 0.9% and were administered via the intraperitoneal route for 3 weeks.

### Phase 1 study design

The Institutional Review Board approved the study, which was conducted according to the provisions of the Declaration of Helsinki and the International Conference on Harmonization Guidelines for Good Clinical Practice. This was an open-label, phase 1, single-arm study registered with ClinicalTrials.gov (identifier NCT00691210). All patients enrolled gave written informed consent. All authors had access to primary data.

The primary objective was to determine maximal tolerated dose (MTD) and dose-limiting toxicity (DLT) of vorinostat and niacinamide in combination. Secondary objectives included describing overall response rate (ORR) (complete remission [CR] plus partial remission [PR]) and duration of response. Response was determined using clinical parameters, computed tomography or positron emission tomography/computed tomography, and bone marrow biopsy, as outlined by the 2007 International Harmonization Project criteria.[34]

Modified Fibonacci dose escalation design was employed using standard 3 + 3 design. Patients received a vorinostat fixed dose of 400 mg orally on days 1 to 14 of a 21-day cycle. Niacinamide was given orally on days 1 through 14 of a 21-day cycle and escalated as follows: 20 mg/kg, 40 mg/kg, 60 mg/kg, 80 mg/kg, and 100 mg/kg. Patients receiving at least 1 dose of the drug were considered evaluable for toxicity (for study flow, see supplemental Figure 1; see the *Blood* Web site). Patients who completed 1 cycle of therapy, defined as receiving >60% of study drugs, were considered evaluable for determination of DLT. All adverse events were evaluated according to the criteria outlined in the National Cancer Institute Common Terminology Criteria for Adverse Events version 3.0. DLTs were defined as follows: grade 4 neutropenia that did not resolve to grade ≤2 within 7 days, any grade 4 thrombocytopenia; any hematologic toxicity that required dose delay of >14 days, and any grade 5. Nonhematologic DLTs were defined as any grade ≥3, with exception of the following: grade 3 nausea, vomiting, diarrhea, or dehydration that occurred with inadequate compliance of supportive care measures; grade 3 acidosis or alkalosis that returned to grade ≤2 within 48 hours; isolated grade 3 elevation of liver function tests or amylase without clinical symptoms that lasted ≤5 days; grade 3 hypocalcemia, hypokalemia, hypomagnesemia, hyponatremia, or hypophosphatemia that responded to intervention; and grade 3 hypercholesterolemia, hypertriglyceridemia, alopecia, constipation, and fatigue.

The MTD was defined as the dose level at which one-third or less of patients experience a DLT. Standard supportive treatment was allowed as clinically indicated including antiemetics, antidiarrheal, antipyretics, antihistamines, analgesics, antibiotics, and blood products.

### Eligibility

Eligible patients were required to have relapsed/refractory biopsy proven lymphoma, of any subtype. Inclusion criteria were as follows: evaluable disease, age ≥18 years, ECOG performance status ≤2, and adequate organ and marrow function. There was no upper limit to the number of prior therapies or stem cell transplantation (SCT). Patients were excluded if they had chemotherapy or radiotherapy within 2 weeks or monoclonal antibodies within 3 months (unless there was evidence of disease progression). Administration of prednisone or the equivalent must have been stabilized to a dose ≤10 mg/day × 7 days. Patients were ineligible if they had central nervous system/leptomeningeal disease, had other uncontrolled intercurrent illness, were pregnant or nursing, had HIV, or have had an allergic reaction attributed to structurally related compounds.

### Response assessment

Response was assessed in accordance with the International Harmonization Project Group 2007 Revised Response Criteria.[34] Efficacy was evaluated after 2 cycles of therapy; thereafter, tumor assessment was performed clinically every 2 to 4 months until progression of disease (POD). All patients were followed for survival and disease progression for 2 years following discontinuation.

### Statistical analysis

***Preclinical studies.*** $IC_{50}$ (half the maximal inhibitory concentration) for each cell line was calculated using the Calcusyn Version 2.0 software (Biosoft).[35]

A

| Compound | t(h) | Cell Line | | | | | | | |
|---|---|---|---|---|---|---|---|---|---|
| | | DLBCL - ABC | | | | DLBCL - GC | | | |
| | | SUDHL2 | Ly10 | Hbl1 | Riva | Ly1 | SUDHL6 | Ly7 | SUDHL4 |
| Niacinamide (mM) | 24 | 14.4 | 17.1 | 19.5 | 47.4 | 8.3 | 13.4 | 13.8 | 16.5 |
| | 48 | 11.9 | 16 | 13.3 | 16.5 | 7.3 | 10.9 | 13.1 | 11.5 |
| | 72 | 13.6 | 18.8 | 13 | 16.1 | 6.5 | 11.7 | 12.8 | 14 |

B

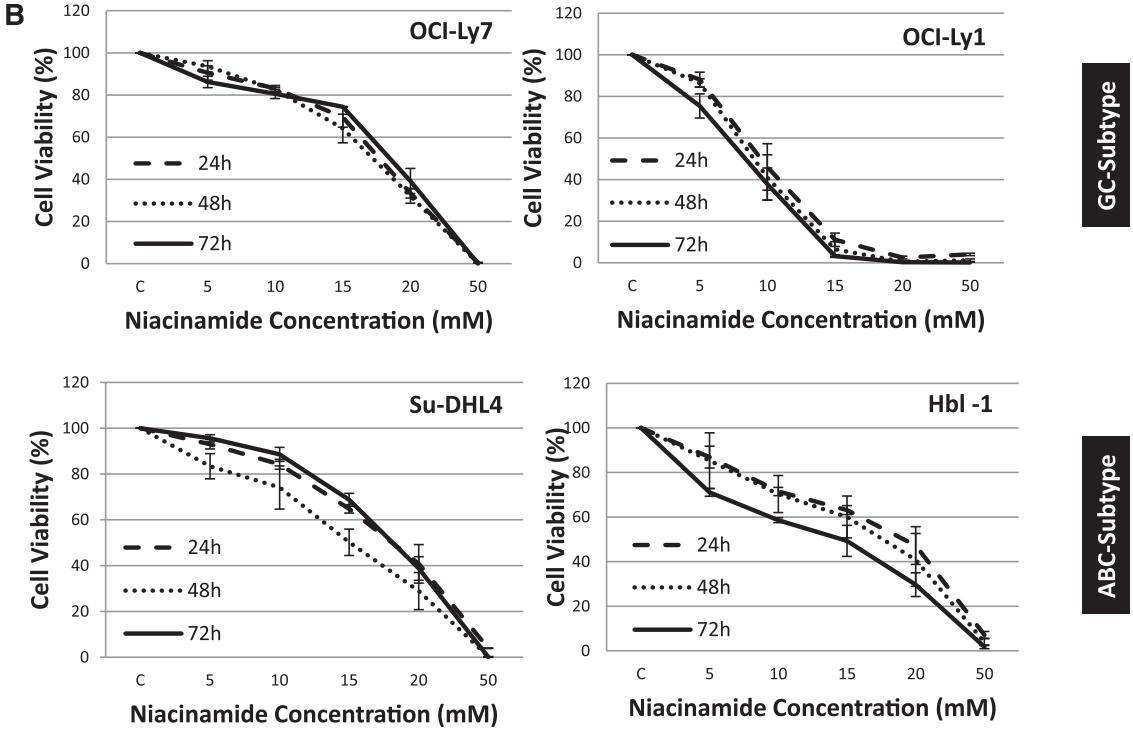


**Figure 1. $IC_{50}$ values: luminometric assays.** (A) Growth inhibition $IC_{50}$ mean values in 8 DLBCL cell lines at 3 time points were explored for niacinamide. (B) Niacinamide induces weak growth inhibition in a spectrum of DLBCL. In 4 DLBCL lines, niacinamide induced concentration, but not time-dependent, growth inhibition. Values represent means expressed as percentages compared with the untreated control; error bars represent standard deviation.

Relative risk ratio (RRR) was used as a model for establishing synergy between 2 drugs. RRR is based on calculating the ratio between the actual value and the expected value (EV). In the case of 2 cytotoxic compounds, EV is calculated by the formula $EV = (N_A \times N_B)/100$, where $N_A$ represents the percentage of viable cells treated with drug A and $N_B$ represents the percentage of viable cells treated with drug B. RRR $<1$ represents a synergistic effect, values equal to 1 indicate the mean additive effect, and values $>1$ represent an antagonistic effect. Significance was determined using unpaired Student *t* test analysis.

For evaluation of the in vivo study, the log-linear mixed model was used to assess the treatment differences in the tumor intensity,[36] calculated as follows: $\text{Log (intensity)} = B_0 + B_1 \text{ time} + B_2 \text{ trt} + B_3 \text{ time} \times \text{trt} + \varepsilon_i + e_{ij}$.

The model assumes that the logarithm of the tumor intensity is linear in time and allows different intercepts and slopes for different treatment groups. Random effect ($\varepsilon_i$) of individual mice was included to account for within-mouse correlation and to help improve the statistical power to assess treatment differences. Because of small sample size, all the hypotheses were tested using the permutation test.[37]

## Results

### Single-agent activity of pan-class DAC inhibitors and niacinamide

Previous experiences in our laboratory have demonstrated that the inhibitory concentration 50% ($IC_{50}$) of the pan-class DAC inhibitors exhibited marked variability depending on the disease recapitulated, duration of exposure, and individual DAC inhibitor.[38] For example, vorinostat exhibited $IC_{50}$ values ranging from 687 to 2100 nM across a panel of lymphoma cell lines, with little difference between GC- and activated B-cell (ABC)-derived lines. In contrast, romidepsin exhibited a range from 2 to 3.6 nM. In this experience, rank ordering the potency of the DAC inhibitors in the most sensitive cell line (OCI-Ly1) would follow romidepsin $>>$ panobinostat $>$ belinostat $>>$ vorinostat.

Niacinamide exhibited weak single-agent activity in DLBCL cell lines, demonstrating a concentration, but not time-dependent, effect (Figure 1A-B). $IC_{50}$ values ranged from 7.3 mM (OCI-Ly1) to 16 mM (OCI-Ly10) across the panel of DLBCL lines.

### Combinations of sirtuin and pan-class DAC inhibitors are synergistic in GC-derived DLBCL cell lines

Using the calculated $IC_{10\text{-}20}$ values from the single-agent concentration effect curves, the synergistic interactions between each of the 4 pan-DAC inhibitors and niacinamide were calculated. Eight cell lines, 4 GC and 4 ABC subtypes, were treated with 1 of 4 pan-DAC inhibitors at the $IC_{10}$ or $IC_{20}$ alone or in combination with niacinamide at 5 or 10 mM (approximating the $IC_{10}$ and $IC_{20}$), and evaluated following 24, 48, and 72 hours of exposure. Figure 2A

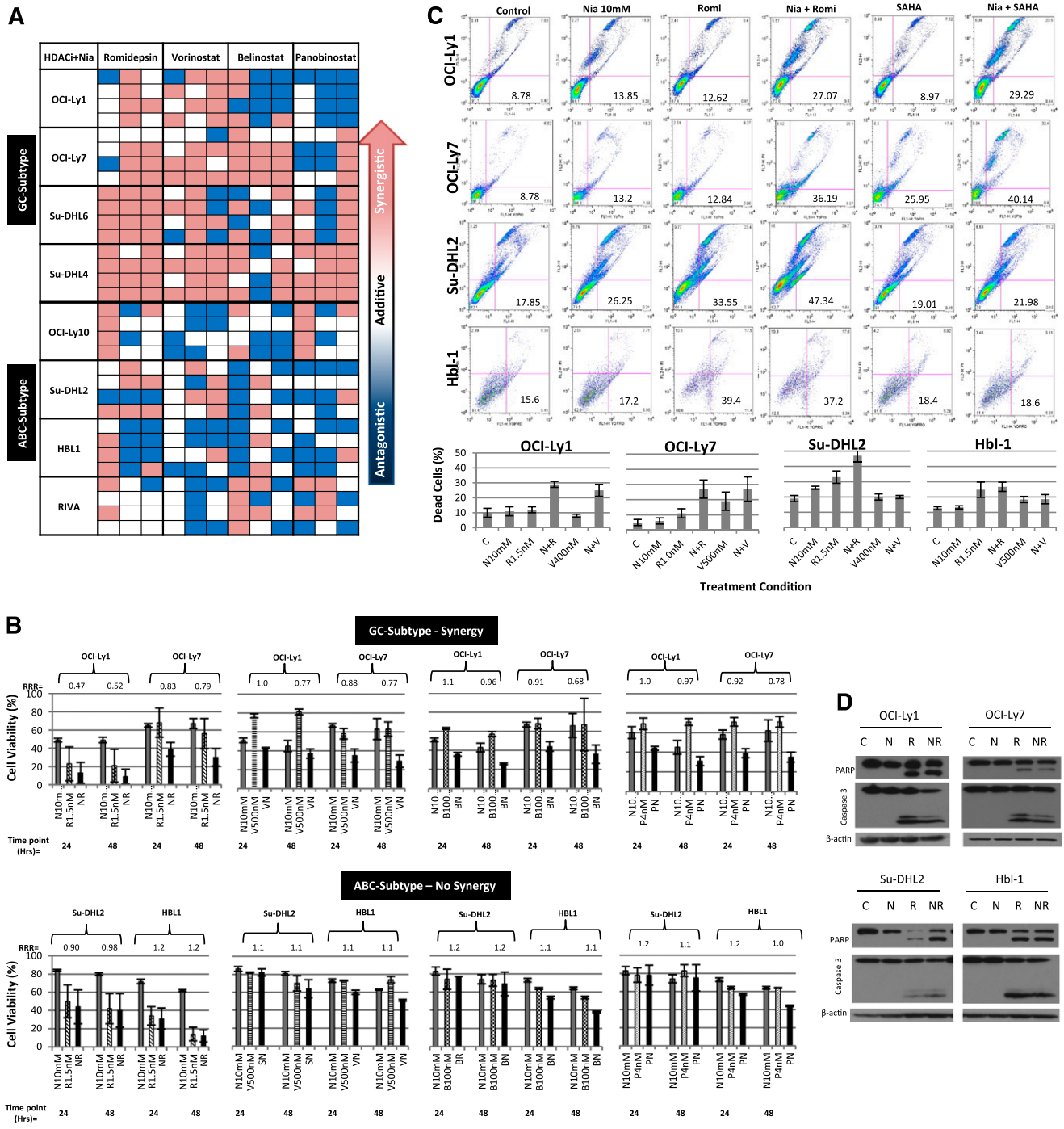


**Figure 2. Synergy between niacinamide and 4 pan-class I/II DAC inhibitors in luminetric assays.** (A) "Heat map" representing synergy coefficients for 8 DLCBL cell lines treated with niacinamide in combination with 1 of 4 pan-class I/II DAC inhibitors: romidepsin, vorinostat, belinostat, or panobinostat. Cells were treated with niacinamide, 5 and 10 mM, in combination with both the $IC_{10}$ and $IC_{20}$ of each pan-DAC inhibitor (romidepsin, 1 nM, 1.5 nM; vorinostat, 400 nM, 500 nM; belinostat, 100 nM, 300 nM; and panobinostat, 2 nM, 4 nM). Cytotoxicity was measured at 24, 48, and 72 hours. Synergistic RRR values $<1$ are represented by red boxes, additive RRR values $= 1$ are represented as white boxes, and antagonistic RRR values $>1$ are represented as blue boxes. GC-derived DLBCL achieved greater synergistic cytotoxicity compared with ABC-derived DLBCL cell lines. (B) Cell viability as compared with controls in 4 DBLCL cell lines treated with niacinamide in combination with 1 of 4 pan-class DAC inhibitors at 24 and 48 hours. Concentrations of drugs were as follows: niacinamide, 10 mM (N); romidepsin, 1.5 nM (R); vorinostat, 500 nM (V); belinostat, 100 nM (B); and panobinostat, 4 nM (P). Each bar represents the mean of 3 experiments expressed as percentages compared with the untreated control; error bars represent standard deviation. (C) Assessment of apoptosis by Yo-Pro-1 and propidium iodide in DLBCL lines. Two GC- and 2 ABC-DLBCL cell lines were incubated with niacinamide (10 mM) alone, pan-class DAC inhibitor alone, either vorinostat or romidepsin, or the combination of niacinamide plus pan-class DAC inhibitor for 48 hours. All cell lines were treated with 10 mM niacinamide; OCI-Ly1, Su-DHL2, and HBL-1 were treated with 1.5 nM romidepsin; OCI-Ly7 was treated with 1.0 nM romidepsin; OCI-Ly1 and Su-DHL2 were treated with 400 nM vorinostat; OCI-Ly7 and HBL-1 with 500 nM vorinostat. Compared with the untreated control, niacinamide or pan-class DAC inhibitor alone resulted in minimal apoptosis. Combination of niacinamide with romidepsin or vorinostat led to increased apoptosis in GC-derived DLBCL cell lines to a greater degree compared with ABC-derived cell lines. (D) PARP and caspase 3 cleavage was demonstrated for cells treated with romidepsin alone and to a greater degree in combination with niacinamide at 24 hours. C, untreated control; N, niacinamide; NR, combination; R, romidepsin.

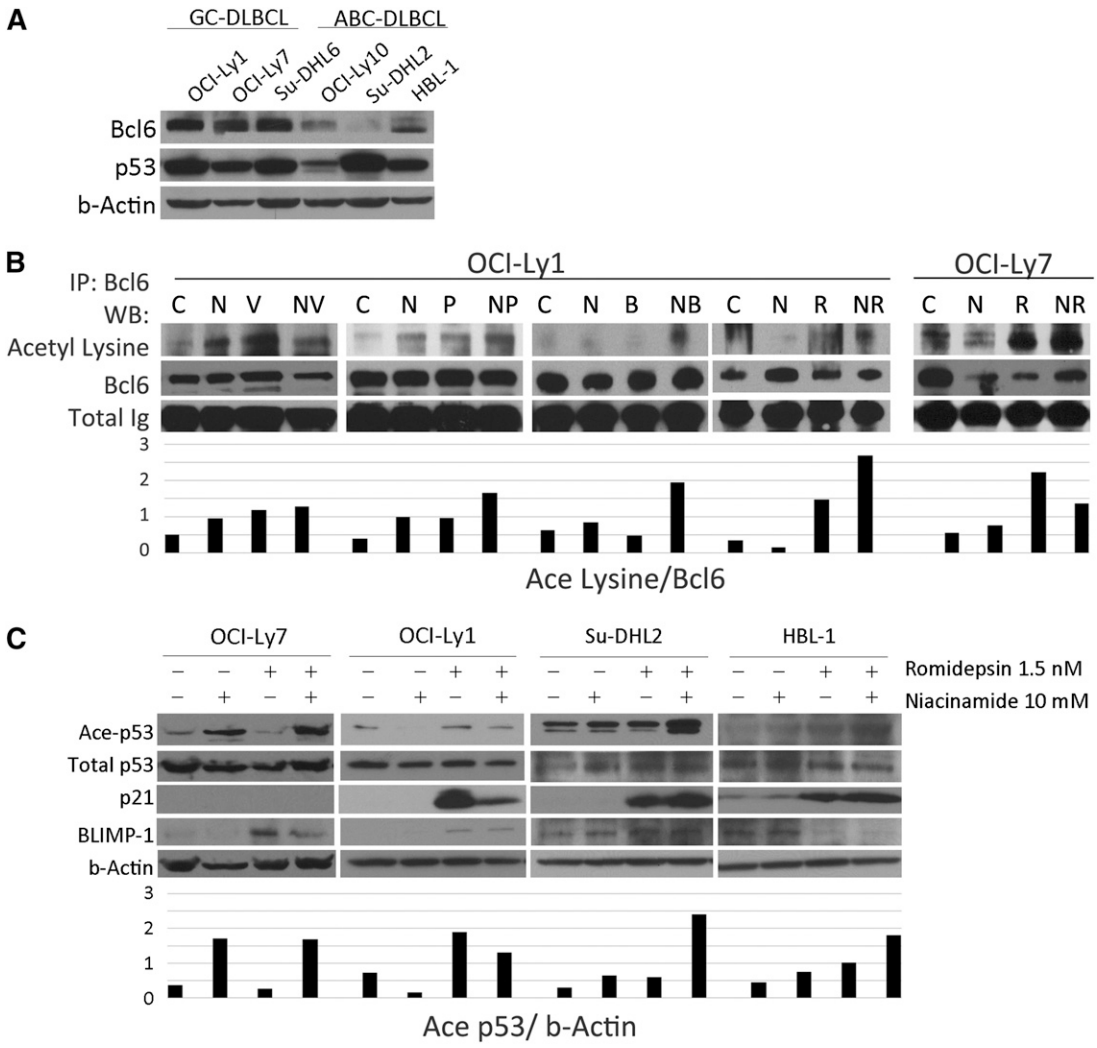


**Figure 3. Acetylation of Bcl6 and p53 in DLBCL lines after treatment with niacinamide and pan-class I/II DAC inhibitor.** (A) Western blot analysis of Bcl6 and p53 in 6 untreated DLBCL cell lines. Bcl6 is expressed to a greater degree in GC- over ABC-subtype DLBCL. (B) Acetylation of Bcl6 in 2 GC-derived DLBCL cell lines treated for 3 hours with niacinamide (N), 10 mM, and/or 1 of 4 pan-class DAC inhibitors: vorinostat (V), 3 uM; panobinostat (P), 15 nM; belinostat (B), 600 nM; or romidepsin (R), 6 nM for OCI-Ly1 and 1.5 nM for OCI-Ly7. Whole cell lysates were analyzed by immunoprecipitation for Bcl6 and Western blot analysis for acetyl lysine. Densitometry analysis was performed on scanned immunoblot images using the ImageJ software (National Institutes of Health). Relative levels of acetylated-Bcl6 were calculated and plotted. (C) Western blot analysis of acetylated-p53, total p53, p21, and Blimp1 in 4 DLBCL cell lines treated with 10 mM niacinamide, 1.5 nM romidepsin, or the combination for 24 hours. OCI-Ly7 does not express p21 at measurable levels at baseline.

depicts a "heat map," where synergy (RRR $<1$) is represented by the red boxes, additivity (RRR $= 1$) by the white boxes, and antagonism (RRR $>1$) by the blue boxes. This representation provides a global view of the drug:drug interactions as a function of cell of origin, DAC inhibitor, and duration of exposure simultaneously. These data demonstrate that the combination of romidepsin and vorinostat consistently produces the greatest synergy with niacinamide in the GC-derived cell lines, compared with belinostat and panobinostat. Nearly all the synergy coefficients calculated for the combination studies of the pan-DAC inhibitors and niacinamide in the GC-derived cell lines were synergistic, whereas the majority of the coefficients of the ABC lines were in the additive to antagonistic range. The histograms presented in Figure 2B depict the synergy coefficients as a function of the drug:drug interaction and cell line. The lowest, most potent, synergy coefficients were observed between romidepsin at 1.5 nM and niacinamide (RRR 0.42-0.52, $P = .018$-$.0006$). In contrast, the majority of the synergy coefficients seen in the ABC-derived lines approximated 1.0. Figure 2C-D presents supporting evidence that combinations of pan-DAC inhibitor and niacinamide increase apoptosis to a greater extent in GC-derived cell lines compared with ABC-derived lines. Collectively, these in vitro data support the conclusion that the combination of pan-DAC inhibitor and sirtuin inhibitor are selectively more cytotoxic in GC-derived DLBCL cell lines. They also support the notion that not all the DAC inhibitors are equal in mediating this synergistic interaction, with vorinostant and romidepsin being more effective in combination with niacinamide.

### Acetylation of both Bcl6 and p53 correlates with the cytotoxicity of pan-DAC and sirtuin inhibition in GC-derived DLBCL cell lines

Overexpression of Bcl6 is known to drive proliferation of GC-derived cell lines and is present, to a lesser extent, in ABC-derived cell lines. Bcl6 recruits the corepressor MTA3 to inhibit Blimp1, the master regulator of plasma cell differentiation, preventing

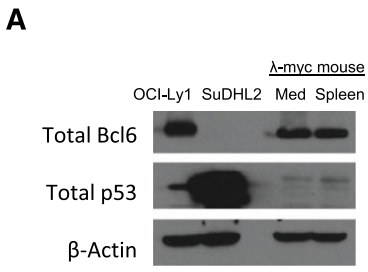


C

| | Treatment Schedules N+R and N→R | | | | | | | |
|---|---|---|---|---|---|---|---|---|
| N+R & N→R | Niacinamide 60 mg/kg | ↓ | ↓ | ↓ | ↓ | ↓ | | |
| N+R | Romidepsin 1.0 mg/kg | ↓ | | | | | | |
| N→R | Romidepsin 1.0 mg/kg | | | ↓ | | | | |
| | Day | 1 | 2 | 3 | 4 | 5 | 6 | 7 |

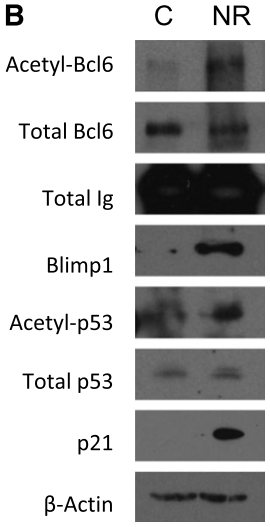


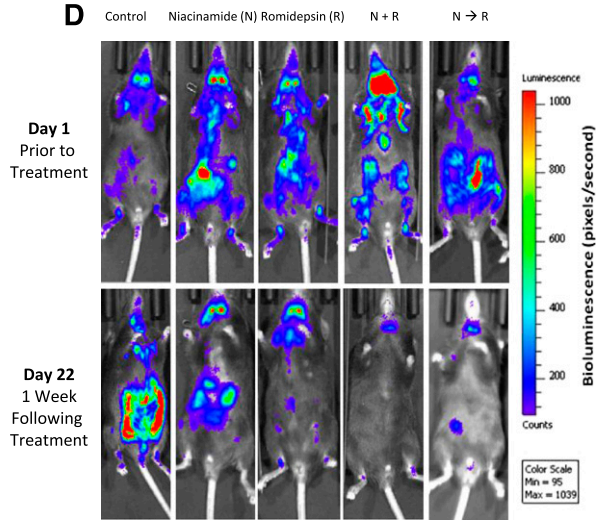


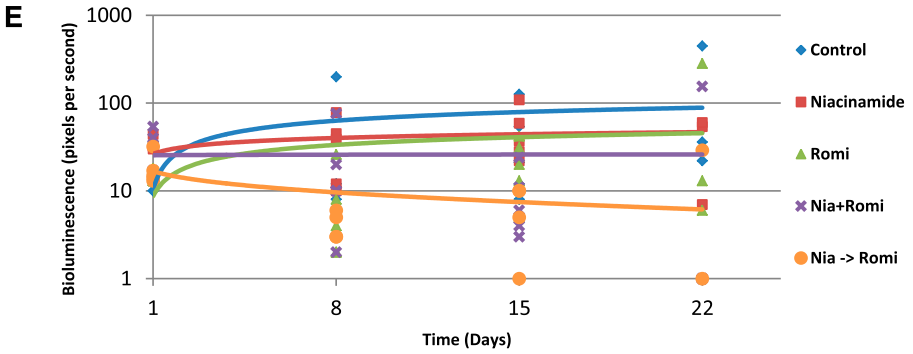


F

| | >10% Wt- Loss | Death- Toxicity | Death- Tumor | Complete Response |
|---|---|---|---|---|
| Control | 0/5 | 0/5 | 1/5 | 0/5 |
| Niacinamide(N) | 1/5 | 0/5 | 3/5 | 0/5 |
| Romidepsin (R) | 0/6 | 1/6 | 3/6 | 0/6 |
| N+R | 1/5 | 1/5 | 1/5 | 2/5 |
| N→R | 0/5 | 1/5 | 1/5 | 1/5 |

G

| Treatment Group | Estimated Rate of Growth |
|---|---|
| Control | +0.04 |
| Niacinamide | +0.022 |
| Romidepsin | -0.003 |
| N + R | -0.045 |
| N → R | -0.007 |

**Figure 4. Romidepsin in combination with niacinamide is effective therapy in a genetically engineered mouse model (GEMM) of spontaneous aggressive B-cell lymphoma expressing Bcl6.** GEMM of a C57BL with λ-MYC overexpressed crossed with a mCherry fluorescent luminescent CD19 was used to assess effectiveness and tolerability of romidepsin in combination with niacinamide in the context of a normal immune system and microenvironment. (A) Whole-cell lysates prepared from the mediastinum and spleen of an untreated λ-MYC overexpressing mouse expresses similar quantities of Bcl6 and p53 as the GC-derived DLBCL cell line, OCI-Ly1, as compared with ABC-derived DLBCL cell line, Su-DHL2. (B) GEMM λ-MYC overexpressing mouse treated with niacinamide (40 mg/kg) and romidepsin (2.3 mg/kg) intraperitoneally and euthanized 5 hours later. Lysates prepared from the lymphoid tissue of the treated mouse and a control mouse were evaluated for acetylated-Bcl6 by immunoprecipitation, and Blimp1, acetylated-p53, total p53, and p21 by Western blot analysis. (C) Treatment schedules for groups of animals receiving both niacinamide and romidepsin. Schedules varied only by the sequence of the 2 drugs, with mice treated according to schedule N + R receiving romidepsin on day 1, and those treated according to schedule N→R receiving romidepsin on day 3. (D) Bioluminescence signal intensity of CD19 luminescence in representative mice from each cohort on day 1 prior to treatment, and day 22, 1 week following completion of treatment. (E) Mice were injected with 150 mg/kg D-luciferin and anesthetized after 5 minutes with a mixture of 2% isofluorane/air. Bioluminescence of each mouse was acquired by IVIS system (Xenogen) and analyzed with Living Image software (Xenogen) as a function of time for each cohort. (F) Summary of the toxicity and response to therapy at day 22 from the start of treatment. (G) Estimated rate of growth of each cohort of mice. The change of log intensity in the N + R cohort is significantly slower than the control cohort ($P \leq .01$).

centroblasts from exiting the GC. Acetylation of Bcl6 has been shown previously to dissociate MTA3 leading to upregulation of Blimp1.[16] Western blots for 6 DLBCL cell lines probed for Bcl6 and p53 confirm that for these cell lines, Bcl6 is more abundant in GC-derived cell lines (OCI-Ly-1, OCI-Ly-7, and Su-DHL-6), whereas there is little to none in the ABC lines (OCI-Ly10, Su-DHL-2, and HBL-1) (Figure 3A). Figure 3B shows acetylated-Bcl6 as a function of treatment with different DAC inhibitors and niacinamide. It demonstrates that combination of pan-DAC inhibitor plus niacniamide increases acetylated-Bcl6. The combination of romidepsin and niacinamide increases accumulation of acetylated-p53 and p21 across the cell lines examined (p21 is not present in OCI-Ly7[31] confirmed by PCR; data not shown). Blimp1 accumulates in cell lines treated with the combination. These data support the fact that the pan-DAC inhibitors and niacinamide lead to accumulation of acetylated-Bcl6 and acetylated-p53, and that these posttranslational modifications are associated with an increase in their downstream genes including p21 and Blimp1.

**Table 1. Patient characteristics**

| Characteristic | N (%) |
|---|---|
| Median age | 43 (range 25-75) |
| Female | 11 (44) |
| **Race/ethnicity** | |
| White (non-Hispanic) | 21 |
| Hispanic | 4 |
| **Histology** | |
| Hodgkin lymphoma (HL) | 12 |
| DLBCL | 4 |
| Follicular lymphoma | 3 |
| Other non-Hodgkin lymphoma (NHL)* | 6 |
| **Prior treatment** | |
| Median # of prior systemic | 4 |
| therapeutic regimens | (range 1-15) |
| Prior autologous SCT | 16 |
| Prior allogeneic SCT | 4 |

*Other NHL histologies included the following: angioimmunoblastic T-cell lymphoma, marginal zone lymphoma, primary mediastinal LBCL, chronic lymphocytic leukemia, anaplastic large cell lymphoma, and mantle cell lymphoma.

### Combined sirtuin and pan-DAC inhibition leads to decreased tumor burden in an in vivo model of aggressive spontaneous lymphoma

To test this drug combination in vivo, a spontaneous double-transgenic mouse model of aggressive B-cell lymphoma developed in our laboratory was used.[33] This model crosses the λ-MYC transgenic mouse with the CD19-CherryLuciferase mouse, producing a mouse that develops spontaneous and bioluminescent aggressive lymphoma in the background of an immunocompetent host. The λ-MYC heterozygous transgenic mice begin to develop lymphadenopathy between 6 and 8 weeks of age and live 38 to 216 days, after which the mice die of progressive disease. Similar to untreated DLBCL observed in patients, these mice develop extensive systemic disease that grows at a logarithimic rate, often difficult to reverse with pharmacologic intervention. Lysates prepared from the mediastinum and spleen were probed for Bcl6 and p53 expression confirming a similar expression pattern to the GC-DLBCL cell line OCI-Ly1(Figure 4A). Figure 4B presents tissue collected from a mouse after treatment with niacinamide and romidepsin. These data confirm that this drug combination results in acetylated-Bcl6, acetylated-p53, and accumulation of Blimp1 and p21, consistent with in vitro experiments. Two different schedules of romidepsin administration were employed to explore the merits of "priming" p53 with a preexposure to niacinamide (Figure 4C). Representative images taken from mice treated with romidepsin and niacinamide demonstrate that the mice treated with the combination have a substantially lower tumor burden compared with control and single-agent cohorts (Figure 4D). Analysis of the relative tumor signal intensities of the entire cohort of animals demonstrates that a combination of niacinamide plus romidepsin yields the most favorable outcome (Figure 4E). The estimated rate of log intensity increase for the control group was 0.04 per day, compared with 0.022, −0.003, −0.045, and −0.007 for the niacinamide, romidepsin, N + R, and N→R cohorts, respectively. Statistically, however, the N + R cohort was the only one that was different from other treatment cohorts ($P \leqslant .01$). The favorable therapeutic effect of the combination is reflected by the fact that CRs were noted only in the combination arms, including N + R (2 CR) and N→R (1 CR). Collectively, these data support the concept that combinations of sirtuin and pan-DAC inhibitor exhibit therapeutic activity in a model of Bcl6+ aggressive B-cell lymphoma compared with untreated and single-agent cohorts. Furthermore, this clearly establishes the on-target effects of this combination, which produces acetylated-Bcl6 and acetylated-p53, and downstream accumulation of Blimp1 and p21. Based on these data, a phase 1 study of this combination was designed for patients with lymphoma.

### Niacinamide plus vorinostat produces meaningful clinical patients' activity in a proof-of-principle phase 1 clinical trial

Twenty-eight patients were screened, and 25 patients enrolled. The patient characteristics are outlined in Table 1. The median age was 43 (range 25-75), 44% were female, and 84% were white. This was a group of heavily pretreated patients. The median number of therapies was 4 (range 1-15), with 17 patients (68%) having had an autologous SCT and 4 (16%) an allogeneic SCT. Seven patients (28%) had GC-derived lymphoma, including 4 with DLBCL and 3 with follicular lymphoma. A range of 1 to 18 cycles was administered. Of the 25 patients evaluable for toxicity, 21 patients were evaluable for DLT, and 21 were evaluated for response assessment (see supplemental Figure 1 for study flowchart).

### DLT and MTD

The treatment was well tolerated. The most significant toxicity was related directly to the number of niacinamide pills. The most common toxicities included fatigue (84%), nausea (80%), diarrhea (72%), and anorexia (56%) (Table 2). In total, there were 12 different grade 3 to 4 toxicities that occurred in 11 patients. There was 1 event in dose cohort 4 (vorinostat, 400 mg; niacinamide, 80 mg/kg) that qualified as a DLT, namely, a grade 3 infection that was presumed pneumonia. Two DLTs occurred at dose level 5 (vorinostat, 400 mg; niacinamide, 100 mg/kg): a grade 4 transaminitis not otherwise explained and a grade 4 hypotension. These events led to the identification of dose cohort 4 (which required 14 tablets of the

**Table 2. Drug toxicities**

| Toxicity | Grade 1 | Grade 2 | Grade 3 | Grade 4 | Total (%) |
|---|---|---|---|---|---|
| Fatigue | 16 | 4 | 1 | | 21 (84) |
| Nausea | 14 | 4 | 2 | | 20 (80) |
| Diarrhea | 16 | 1 | 1 | | 18 (72) |
| Anorexia | 11 | 2 | 1 | | 14 (56) |
| Vomiting | 10 | 1 | 2 | | 13 (52) |
| Constipation | 10 | | | | 10 (40) |
| Flushing | 7 | | | | 7 (28) |
| Fever | 6 | | | | 6 (24) |
| Thrombocytopenia | 2 | 1 | 3 | | 6 (24) |
| Headache | 5 | | | | 5 (20) |
| Anemia | | 2 | 2 | | 4 (16) |
| Cramping (abdominal) | 4 | | | | 4 (16) |
| Creatinine | 1 | 3 | | | 4 (16) |
| Dizziness | 4 | | | | 4 (16) |
| Alanine aminotransferase | | 1 | 1 | 1 | 3 (12) |
| Aspartate aminotransferase | | 2 | | 1 | 3 (12) |
| Cough | 3 | | | | 3 (12) |
| Edema | 3 | | | | 3 (12) |
| Gas | 3 | | | | 3 (12) |
| Infection | | | 3 | | 3 (12) |
| Metallic taste | 3 | | | | 3 (12) |
| Neutropenia | | 2 | | 1 | 3 (12) |
| Pain (abdominal) | 3 | | | | 3 (12) |
| Pruritis | 1 | 2 | | | 3 (12) |
| Rash | 2 | 1 | | | 3 (12) |

Additional significant toxicities that occurred in <10% of patients: 2 patients had grade 2 zoster, 1 patient had a grade 4 hypotension, and 1 patient had grade 3 syncope.

**Table 3. Overall response rates**

| Disease (n = # of evaluable patients) | CR (%) | PR (%) | ORR (%) | SD (%) | POD (%) |
|---|---|---|---|---|---|
| NHL (n = 11) | 2 (18) | 0 (0) | 2 (18) | 5 (46) | 4 (36) |
| HL (n = 10) | 0 (0) | 3 (30) | 3 (30) | 7 (70) | 0 (0) |
| Overall (n = 21) | 2 (10) | 3 (14) | 5 (24) | 12 (57) | 4 (19) |

CR is 100% reduction in disease, PR is >50% reduction in disease, and SD is <50% disease reduction.

SD, stable disease.

vitamin and 2 tablets of vorinostat) as the MTD. There were 2 deaths that occurred within the safety follow-up period (30 days following the last dose of therapy); none of these events was related to the study drugs. The first was in a patient with HL who had completed 5 cycles. The sixth cycle was held due to transaminitis. Liver biopsy revealed a new diagnosis of T-cell lymphoma. The patient expired 32 days after his last dose of treatment due to liver failure secondary to T-cell lymphoma. The second death occurred in a heavily pretreated and multiply relapsed chronic lymphocytic leukemia patient who received 7 days of therapy and developed rapid POD with a briskly doubling white blood cell count. Immediately after withdrawing due to POD, the patient received dexamethasone, pentostatin, and cytoxan. Following treatment, the patient presented to a local emergency room with chest pain and suffered a myocardial infarction expiring within 3 hours of presentation. These events were reviewed by the data monitoring safety committee and were deemed to be unrelated to study drugs. Aside from the difficulty patients had ingesting a large number of niacinamide pills, the treatment was very well tolerated.

### Efficacy

The ORR was 24%, with 2 CRs and 3 PRs (Table 3). One CR and 2 PRs were obtained after only 2 cycles of treatment. In the first cohort, a patient with GC-DLBCL who had 5 prior chemotherapy regimens, including an allogeneic SCT, achieved a CR maintained for 18 weeks. The second CR was obtained after 10 cycles, and maintained for 13 weeks in a patient with marginal zone lymphoma who had received 3 prior regimens. All PRs were achieved in patients with HL who had received 6 to 10 prior regimens and autologous SCT, with 1 patient also having had an allogeneic SCT. PRs were maintained for 4 to 13 weeks. Twelve patients achieved SD (57%). Two of these patients were very close to a PR, with 1 patient achieving 45% and another 30% reduction in tumor burden.

## Discussion

Our rapidly increasing understanding of the molecular basis for lymphomagenesis has created new opportunities to treat these diseases. Work by several groups using gene expression profiling has begun to organize many subtypes of lymphoma into discrete molecular phenotypes.[1,2] Work by Shipp et al has identified distinct subsets of DLBCL, including one that is comparatively more addicted to B-cell receptor (BCR) signaling, which appears more sensitive to BCR inhibition via SYK inhibitors.[39,40] Staudt et al have demonstrated that DLBCL can be subcategorized into 3 molecular subtypes: GC derived, ABC derived, and type 3, or primary mediastinal large B-cell lymphoma. DLBCLs derived from the ABC phenotype are driven by BCR signaling and NF-κB, whereas GC-derived lymphomas appear more dependent on Bcl6. This classification carries prognostic ramifications, with the ABC-derived DLBCL carrying a worse prognosis. Staudt's group has demonstrated that the combination of BTK inhibition and lenalidomide synergistically interacts to inhibit NF-κB, providing a molecular rationale for designing clinical trials for ABC-derived DLBCL.[41-43] One recent clinical experience suggests that development of a chemotherapy regimen targeting NF-κB may be more sensitive in ABC- over GC-derived DLBCL. Dunleavy et al have demonstrated that the addition of bortezomib to DA-EPOCH can overcome the negative impact of ABC-DLBCL, by inhibiting NF-κB.[44] Similarly, attempts have been made at targeting Bcl6 in GC-derived DLBCL. Melnick et al have developed a Bcl6 peptide inhibitor, which is currently in early stages of clinical development.[9] Although promising, these strategies are yet to be validated in a clinical setting.

The strategy evaluated here proposes employing a single class of epigenetic drugs to modulate the posttranslational state of 2 transcription factors (Bcl6:p53) that directly interface in a pathological fashion known to drive GC-derived DLBCL. Bereshchenko et al demonstrated that the transcriptional repressor effects of Bcl6 can be abrogated by trichostatin A and niacinamide. Fujita et al confirmed this and demonstrated that acetylated-Bcl6 led to upregulation of Blimp1 and subsequent differentiation. Despite this rationale, clinical trials evaluating DAC inhibitors alone in DLBCL have not been successful. Crump et al studied vorinostat at 300 mg twice daily for 3 days out of 7 in 18 patients with relapsed DLBCL.[29] The ORR was 5% (1 CR + 1 SD). As a single agent, vorinostat is relatively inert in DLBCL. Likewise, there is no expectation that niacinamide would be cytotoxic in DLBCL.

The data presented here support the concept that an epigenetic-based approach can modulate Bcl6 in a therapeutic fashion, resulting in apoptosis of GC-derived DLBCL. Treatment of a large panel of DLBCL cell lines demonstrated a weak single-agent effect of niacinamide ($IC_{50}$ 7-17 mM). Addition of a pan-DAC inhibitor (romidepsin, vorinostat, belinostat, or panobinostat) led to synergistic cytotoxicity predominantly restricted to GC-derived DLBCL. This combination led to acetylation of Bcl6 and p53 and modulation of the downstream targets p21 and Blimp1. Utilization of a bioluminescent spontaneous aggressive B-cell lymphoma murine model allowed evaluation of romidepsin and niacinamide in the background of an intact microenvironment and immune system. Mice treated with the combination exhibited greater reduction of tumor volume, increased acetylation of Bcl6 and p53, and increased p21 and Blimp1. The ability to assay for acetylated-Bcl6 and acetylated-p53, as well as the downstream effects of the posttranslational modification, opens the possibility of using this as a biomarker for response.

Based on the preclinical experiments discussed previously, a phase 1 clinical trial of vorinostat in combination with niaciniamide in patients with relapsed or refractory lymphoma was conducted, demonstrating an ORR of 24%. This was an unselected and extraordinarily heavily pretreated group of patients, most having received an autologous SCT, allogeneic SCT, or both. Additionally, 12 of 21 patients (57%) experienced stabilization of their aggressive disease.

Ongoing efforts are focused on optimizing biochemical effects of these drugs and determining if isoform-selective DAC inhibitors may more efficiently modulate Bcl6 and p53. Data suggest that vorinostat and niacinamide are among the weaker of the available agents. Hypothetically, inhibiting Bcl6 and activating p53 could sensitize cells to DNA-damaging drugs, like etoposide. If confirmed in ongoing experiments, it is conceivable that such approaches could be used to sensitize GC-derived DLBCL to conventional chemotherapy, as has been demonstrated with the addition of bortezomib to DA-EPOCH. These strategies, as validated with other emerging drugs

such as ibrutinib[45] and lenolidomide,[46] will likely lead to tailoring chemotherapy regimens to the individual patient's molecular phenotype.

## Acknowledgments

The authors thank Riccardo Dalla-Favera for providing the λ-MYC mouse vector and cell lines, as well as Laura Pasqaulucci for providing technical support for immunoprecipitation assays.

This work was supported by the Amos Medical Faculty Development Program of the American Society of Hematology and Robert Wood Johnson Foundations and the Gabriele's Angel Cancer Research Award (J.E.A.), and Leukemia & Lymphoma Society (grant LLS 7017-09) (O.A.O.).

## Authorship

Contribution: J.E.A. performed all experiments; J.E.A. and O.A.O. designed the study, analyzed and interpreted the data, and wrote the paper; J.E.A., E.N., J.Z., and O.A.O. performed clinical research; S.C.-G. collected data; L.S. contributed to the in vivo experiments; M.K., E.M., and P.J. contributed to the in vitro experiments; and Y.W. conducted the statistical analysis.

Conflict-of-interest disclosure: Merck supplied investigational drug and financial support for the clinical trial (O.A.O.). The remaining authors declare no competing financial interests.

Correspondence: Jennifer E. Amengual, 51 W 51st St, Suite 200, New York, NY 10019; e-mail: jea2149@columbia.edu.

## References

1. Alizadeh AA, Eisen MB, Davis RE, et al. Distinct types of diffuse large B-cell lymphoma identified by gene expression profiling. *Nature.* 2000; 403(6769):503-511.
2. Abramson JS, Shipp MA. Advances in the biology and therapy of diffuse large B-cell lymphoma: moving toward a molecularly targeted approach. *Blood.* 2005;106(4):1164-1174.
3. Ye BH, Lista F, Lo Coco F, et al. Alterations of a zinc finger-encoding gene, BCL-6, in diffuse large-cell lymphoma. *Science.* 1993;262(5134): 747-750.
4. Chang CC, Ye BH, Chaganti RS, Dalla-Favera R. BCL-6, a POZ/zinc-finger protein, is a sequence-specific transcriptional repressor. *Proc Natl Acad Sci USA.* 1996;93(14):6947-6952.
5. Phan RT, Dalla-Favera R. The BCL6 proto-oncogene suppresses p53 expression in germinal-centre B cells. *Nature.* 2004;432(7017): 635-639.
6. Ranuncolo SM, Polo JM, Dierov J, et al. Bcl-6 mediates the germinal center B cell phenotype and lymphomagenesis through transcriptional repression of the DNA-damage sensor ATR. *Nat Immunol.* 2007;8(7):705-714.
7. Pasqualucci L, Bereshchenko O, Niu H, et al. Molecular pathogenesis of non-Hodgkin's lymphoma: the role of Bcl-6 [published correction appears in *Leuk Lymphoma.* 2013;54(5):1121]. *Leuk Lymphoma.* 2003;44(suppl 3):S5-S12.
8. Phan RT, Saito M, Basso K, Niu H, Dalla-Favera R. BCL6 interacts with the transcription factor Miz-1 to suppress the cyclin-dependent kinase inhibitor p21 and cell cycle arrest in germinal center B cells. *Nat Immunol.* 2005;6(10):1054-1060.
9. Polo JM, Dell'Oso T, Ranuncolo SM, et al. Specific peptide interference reveals BCL6 transcriptional and oncogenic mechanisms in B-cell lymphoma cells. *Nat Med.* 2004;10(12): 1329-1335.
10. Luo J, Su F, Chen D, Shiloh A, Gu W. Deacetylation of p53 modulates its effect on cell growth and apoptosis. *Nature.* 2000;408(6810):377-381.
11. Niu H, Ye BH, Dalla-Favera R. Antigen receptor signaling induces MAP kinase-mediated phosphorylation and degradation of the BCL-6 transcription factor. *Genes Dev.* 1998;12(13): 1953-1961.
12. Bereshchenko OR, Gu W, Dalla-Favera R. Acetylation inactivates the transcriptional repressor BCL6. *Nat Genet.* 2002;32(4):606-613.
13. Kovacs JJ, Murphy PJM, Gaillard S, et al. HDAC6 regulates Hsp90 acetylation and chaperone-dependent activation of glucocorticoid receptor. *Mol Cell.* 2005;18(5):601-607.
14. Chen Lf, Fischle W, Verdin E, Greene WC. Duration of nuclear NF-kappaB action regulated by reversible acetylation. *Science.* 2001; 293(5535):1653-1657.
15. Parekh S, Polo JM, Shaknovich R, et al. BCL6 programs lymphoma cells for survival and differentiation through distinct biochemical mechanisms. *Blood.* 2007;110(6):2067-2074.
16. Fujita N, Jaye DL, Geigerman C, et al. MTA3 and the Mi-2/NuRD complex regulate cell fate during B lymphocyte differentiation. *Cell.* 2004;119(1): 75-86.
17. Vaziri H, Dessain SK, Ng Eaton E, et al. hSIR2 (SIRT1) functions as an NAD-dependent p53 deacetylase. *Cell.* 2001;107(2):149-159.
18. Bernier J, Stratford MR, Denekamp J, et al. Pharmacokinetics of nicotinamide in cancer patients treated with accelerated radiotherapy: the experience of the Co-operative Group of Radiotherapy of the European Organization for Research and Treatment of Cancer. *Radiother Oncol.* 1998;48(2):123-133.
19. Dragovic J, Kim SH, Brown SL, Kim JH. Nicotinamide pharmacokinetics in patients. *Radiother Oncol.* 1995;36(3):225-228.
20. Nahimana A, Attinger A, Aubry D, et al. The NAD biosynthesis inhibitor APO866 has potent antitumor activity against hematologic malignancies. *Blood.* 2009;113(14):3276-3286.
21. Guarente L. Diverse and dynamic functions of the Sir silencing complex. *Nat Genet.* 1999;23(3):281-285.
22. Bitterman KJ, Anderson RM, Cohen HY, Latorre-Esteves M, Sinclair DA. Inhibition of silencing and accelerated aging by nictinomide, a putative negative regulator of yeast sir2 and human SIRT1. *J Biol Chem.* 2002;277(47):45099-45107.
23. Heltweg B, Gatbonton T, Schuler AD, et al. Antitumor activity of a small-molecule inhibitor of human silent information regulator 2 enzymes. *Cancer Res.* 2006;66(8):4368-4377.
24. O'Connor OA, Heaney ML, Schwartz L, et al. Clinical experience with intravenous and oral formulations of the novel histone deacetylase inhibitor suberoylanilide hydroxamic acid in patients with advanced hematologic malignancies. *J Clin Oncol.* 2006;24(1):166-173.
25. Duvic M, Talpur R, Ni X, et al. Phase 2 trial of oral vorinostat (suberoylanilide hydroxamic acid, SAHA) for refractory cutaneous T-cell lymphoma (CTCL). *Blood.* 2007;109(1):31-39.
26. Piekarz RL, Frye R, Turner M, et al. Phase II multi-institutional trial of the histone deacetylase inhibitor romidepsin as monotherapy for patients with cutaneous T-cell lymphoma. *J Clin Oncol.* 2009;27(32):5410-5417.
27. Woo S, Gardner ER, Chen X, et al. Population pharmacokinetics of romidepsin in patients with cutaneous T-cell lymphoma and relapsed peripheral T-cell lymphoma. *Clin Cancer Res.* 2009;15(4):1496-1503.
28. Ellis L, Pan Y, Smyth GK, et al. Histone deacetylase inhibitor panobinostat induces clinical responses with associated alterations in gene expression profiles in cutaneous T-cell lymphoma. *Clin Cancer Res.* 2008;14(14):4500-4510.
29. Crump M, Coiffier B, Jacobsen ED, et al. Phase II trial of oral vorinostat (suberoylanilide hydroxamic acid) in relapsed diffuse large-B-cell lymphoma. *Ann Oncol.* 2008;19(5):964-969.
30. Marchi E, Paoluzzi L, Scotto L, et al. Pralatrexate is synergistic with the proteasome inhibitor bortezomib in in vitro and in vivo models of T-cell lymphoid malignancies. *Clin Cancer Res.* 2010; 16(14):3648-3658.
31. Shaffer AL, Lin KI, Kuo TC, et al. Blimp-1 orchestrates plasma cell differentiation by extinguishing the mature B cell gene expression program. *Immunity.* 2002;17(1):51-62.
32. Paoluzzi L, Gonen M, Gardner JR, et al. Targeting Bcl-2 family members with the BH3 mimetic AT-101 markedly enhances the therapeutic effects of chemotherapeutic agents in in vitro and in vivo models of B-cell lymphoma. *Blood.* 2008;111(11): 5350-5358.
33. Scotto L, Kruithof-de Julio M, Paoluzzi L, et al. Development and characterization of a novel CD19CherryLuciferase (CD19CL) transgenic mouse for the preclinical study of B-cell lymphomas. *Clin Cancer Res.* 2012;18(14):3803-3811.
34. Cheson BD, Pfistner B, Juweid ME, et al; International Harmonization Project on Lymphoma. Revised response criteria for malignant lymphoma. *J Clin Oncol.* 2007;25(5):579-586.
35. Zhao L, Wientjes MG, Au JLS. Evaluation of combination chemotherapy: integration of nonlinear regression, curve shift, isobologram, and combination index analyses. *Clin Cancer Res.* 2004;10(23):7994-8004.
36. Lindstrom ML, Bates DM. Nonlinear mixed effects models for repeated measures data. *Biometrics.* 1990;46(3):673-687.
37. Welch WJ. Construction of permutation tests. *J Am Stat Assoc.* 1990;85(411):693-698.
38. Kalac M, Scotto L, Marchi E, et al. HDAC inhibitors and decitabine are highly synergistic and associated with unique gene-expression and epigenetic profiles in models of DLBCL. *Blood.* 2011;118(20):5506-5516.
39. Savage KJ, Monti S, Kutok JL, et al. The molecular signature of mediastinal large B-cell lymphoma differs from that of other diffuse large B-cell lymphomas and shares features with classical Hodgkin lymphoma. *Blood.* 2003; 102(12):3871-3879.

40. Friedberg JW, Sharman J, Sweetenham J, et al. Inhibition of Syk with fostamatinib disodium has significant clinical activity in non-Hodgkin lymphoma and chronic lymphocytic leukemia. *Blood.* 2010;115(13):2578-2585.

41. Davis RE, Ngo VN, Lenz G, et al. Chronic active B-cell-receptor signalling in diffuse large B-cell lymphoma. *Nature.* 2010;463(7277): 88-92.

42. Yang Y, Shaffer AL III, Emre NCT, et al. Exploiting synthetic lethality for the therapy of ABC diffuse large B cell lymphoma. *Cancer Cell.* 2012;21(6):723-737.

43. Advani RH, Buggy JJ, Sharman JP, et al. Bruton tyrosine kinase inhibitor ibrutinib (PCI-32765) has significant activity in patients with relapsed/ refractory B-cell malignancies. *J Clin Oncol.* 2013; 31(1):88-94.

44. Dunleavy K, Pittaluga S, Czuczman MS, et al. Differential efficacy of bortezomib plus chemotherapy within molecular subtypes of diffuse large B-cell lymphoma. *Blood.* 2009; 113(24):6069-6076.

45. Wilson WH, Gerecitano JF, Goy A, et al. The Bruton's tyrosine kinase (BTK) inhibitor, ibrutinib (PCI-32765), has preferential activity in the ABC subtype of relapsed/refractory de novo diffuse large B-cell lymphoma (DLBCL): interim results of a multicenter, open-label, phase 2 study [abstract]. *Blood.* 2012;120(21). Abstract 686.

46. Nowakowski GS, LaPlant BR, Reeder C, et al. Combination of lenalidomide with R-CHOP (R2CHOP) is well-tolerated and effective as initial therapy for aggressive B-cell lymphomas—a phase II study [abstract]. *Blood.* 2012;120(21). Abstract 689.